# System-theoretic Framework for Intent Sharing in Cooperative Adaptive Cruise Control

Jing Li, Di Liu, *Member, IEEE*, Simone Baldi, *Senior Member, IEEE*, and Wei Liu

***Abstract*—The vast majority of protocols for connected automated vehicles are based on *status* sharing, i.e., communication of the current vehicle state among neighboring vehicles. Only recently the idea of *intent* sharing has been put forward, where not only the current state, but also the vehicle intention in the near future can be communicated. In the context of Cooperative Adaptive Cruise Control (CACC), this work provides a system-theoretic framework for intent sharing through the lens of output regulation. We present analytical results showing two fundamental aspects of CACC with intent sharing: a) when vehicle-to-vehicle communication is reliable, intent sharing provides no benefits over status sharing, as both sharing paradigms result in the same protocol; b) intent sharing becomes beneficial when vehicle-to-vehicle communication is unreliable, in which case the latest communicated intent can be used to reconstruct the missing information of the neighboring vehicle in the near future. Together with theoretical analysis, numerical validations with synthetic and real-world data are provided, where the benefits of CACC with the proposed implementation of intent sharing are shown against several state-of-the-art CACC protocols.**

***Index Terms*—Connected Automated Vehicles (CAVs), Cooperative Adaptive Cruise Control (CACC), unreliable communication, intent sharing, status sharing, output regulation.**

## I. Introduction

THE progress of information and communication technology is behind several innovations in the field of Connected Automated Vehicles (CAVs) [1]–[3]. A key innovation is the evolution from Adaptive Cruise Control (ACC) to Cooperative Adaptive Cruise Control (CACC), where the on-board sensing of ACC is enhanced with vehicle-to-vehicle (V2V) communication. As compared to ACC, a CACC protocol better exploits the connectivity of CAVs. Several studies have shown that CACC-equipped vehicles provide several advantages over ACC-equipped vehicles, such as smaller inter-vehicle gaps, improved stability of the vehicle string, prompt collision avoidance, among others [4]–[7]. However, because of the reliance on V2V communication, any CACC protocol is inherently subject to unreliability of the wireless communication channel [8]–[10], requiring proper methods to handle such communication constraints.

### A. Related work on communication constraints in CACC

The capacity and reliability of the wireless communication channel can be at stake if a large number of CAVs is deployed on the road. As a result, any CACC protocol needs a module aiming to recover a good level of performance in case of communication failures [11]–[13]. There are two main approaches with which CACC protocols can deal with communication failures. The first approach is to switch from the CACC mode to the ACC mode, which only relies on on-board sensing: an example is the gracefully degraded CACC [13], among other solutions inspired by this idea. A second approach is to design an observer to reconstruct the missing V2V information, with representative examples being [14], [15].

No matter which of the two approaches is used, a certain level of performance degradation of CACC should be accepted in case of unreliable communication. A good design should reduce such degradation as much as possible. For the approaches based on switching between CACC and ACC, the ACC mode can still be designed to achieve desirable properties like string stability and collision avoidance [16], [17], but the missing V2V information will inevitably reduce the ideal performance of CACC with perfect communication. In addition, the switching should be carefully managed to ensure a seamless transition between the two modes [18]. Meanwhile, the approaches based on observers are bound to degrade or fail if the assumptions used to design the observer are not met. Such assumptions include parametric structure of the missing information, homogeneity of the vehicle dynamics, small measurement noises, known upper bounds on the uncertainties. For example, estimating the predecessor acceleration via numerical differentiation from on-board sensors of the follower vehicle [19] assumes small measurement noises, whereas methods based on bounds for the inter-vehicle gap [20] assume a priori known bounds for the acceleration of the predecessor vehicle. In summary, reducing the performance degradation in case of unreliable communication remains an open problem in several V2V protocols for CAVs.

### B. Related work on status-sharing and intent-sharing

Most V2V protocols including the aforementioned CACC protocols are based on *status* sharing, i.e., communication of

This work was partially supported by the National Natural Science Foundation of China under Grants No. 62573115, 6251101378, and 72301228, by Jiangsu Provincial Scientific Research Center of Applied Mathematics No. BK20233002, by Guangdong Basic and Applied Basic Research Fund No. 2023A1515012266, by UKRI Research and Innovation No. EP/Z002214/1, and by Horizon Europe Marie Sklodowska-Curie Action No. 101146446. *(corresponding authors: Simone Baldi and Wei Liu)*
J. Li is with Department of Aeronautical and Aviation Engineering, The Hong Kong Polytechnic University, Hong Kong, China, and with Self-Organizing Mobility Control and Learning Lab, School of Mathematics, Southeast University, Nanjing 210096, China (jing24.li@connect.polyu.hk)
D. Liu is with Self-Organizing Mobility Control and Learning Lab, School of Mathematics, Southeast University, Nanjing 210096, China, and also with the Department of Electrical and Electronic Engineering, Imperial College, London SW7 2BT, United Kingdom (di.liu@imperial.ac.uk)
S. Baldi is with Self-Organizing Mobility Control and Learning Lab, School of Mathematics, Southeast University, Nanjing 210096, China (s.baldi@seu.edu.cn)
W. Liu is with Department of Aeronautical and Aviation Engineering, The Hong Kong Polytechnic University, Hong Kong, China (wei.w.liu@polyu.edu.hk)

the current vehicle state among neighboring vehicles. Recently, an enhanced V2V paradigm has been proposed based on *intent* sharing [21]–[23], where not only the current state, but also the intention in the near future can be communicated among neighboring vehicles. As this paradigm currently does not involve CACC, it is worth studying how intent sharing can be implemented in a CACC protocol. The intent should not be confused with the prediction over a short horizon used in predictive CACC [24]–[29]. The prediction in predictive CACC protocols is calculated on-board by the follower vehicle via observers [24]–[26] or via neural networks [27]–[29]. On the other hand, the intent is provided to the follower by the predecessor vehicle.

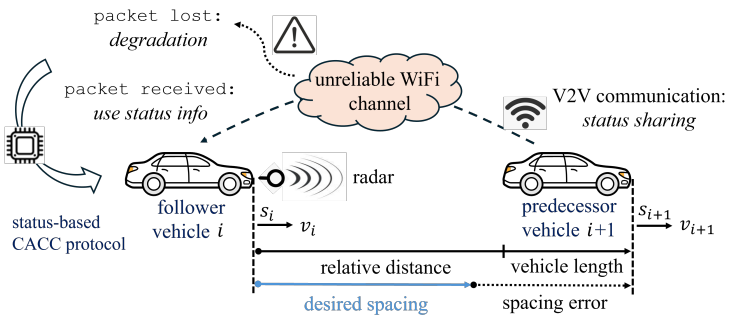


(a) CACC protocol with status sharing

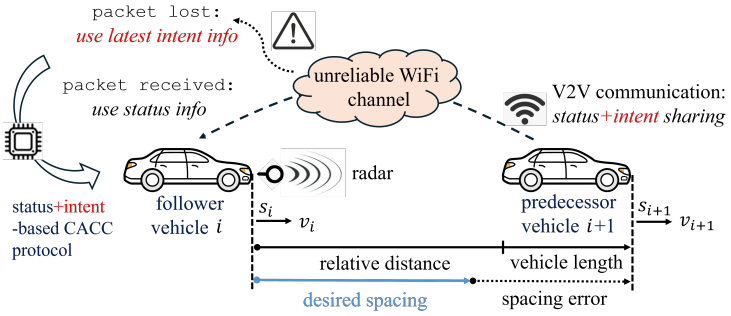


(b) CACC protocol with intent sharing (proposed)

Fig. 1: CACC protocol under unreliable communication: (a) with status sharing, lost communication inevitably leads to performance degradation; (b) with intent sharing, the latest communicated intent can be used to reconstruct the missing information during lost communication periods.

A genuine intent-sharing framework should be based on a prediction calculated by the predecessor vehicle and communicated to the follower. Most importantly, the follower vehicle should make use of the intent information in a way that can be seamlessly integrated with the status information. All these points provide open problems in the field, which are addressed in this study.

### C. Contributions of this study

The main contribution of this work is designing the first intent-sharing framework for CACC vehicle platooning, from the system-theoretic perspective of output regulation. Output regulation is a fundamental problem in control theory, referring to the problem of making a regulated output track the signals generated by an exosystem model [30]–[32]. In the context of CACC, the output to be regulated is the spacing error, while the behavior of the predecessor vehicle (namely, its acceleration) is regarded as generated by an exosystem. By looking at such exosystem as a model for the intent of the predecessor, the goal of output regulation is to make the follower vehicle track the signals generated by such intent model. Under this perspective, the framework in this work provides three major new insights into intent sharing, summarized below.

- *Is intent sharing always beneficial?* One may think that, thanks to the additional future information, intent sharing is always beneficial over status sharing. The output regulation perspective allows to show that when communication is reliable, CACC with intent sharing provides *no* benefits over CACC with status sharing: in fact, Theorem 1 in this work states that, with reliable communication, the CACC intent-sharing protocol takes the same form of a well-known CACC status-sharing protocol in the literature. This is because reliable communication allows to reconstruct the intent from the status information.
- *When is intent sharing beneficial?* Intent sharing becomes advantageous when communication is unreliable. In this case, the result presented in Theorem 2 of this work uses the latest communicated intent to recover the missing information in the near future (refer to Fig. 1). This is intrinsically different from predictive CACC only using on-board sensing: the reconstruction of the missing information we propose is based on previously communicated intent signals along with on-board sensing.
- *How to communicate the intent?* With the proposed output regulation perspective, the intent takes the form of a state matrix internally calculated by the predecessor. The fact that the predecessor generates its own intent marks a difference with standard output regulation literature where the exosystem model is a priori known, either to all or to some agent [33]–[35]. In our case, even the predecessor vehicle does not know a priori its intent model and must generate it. Theorem 3 of this work provides a design allowing the predecessor vehicle to generate its own intent.

Along with the system-theoretic aspects, two additional practical aspects of the proposed design are worth being remarked. First, the proposed intent-sharing framework is designed to be seamlessly integrated with status sharing: namely, the intent-sharing CACC protocol is designed to have the same structure as the CACC status-sharing protocol. Second, the proposed intent-sharing framework is communication-efficient, as it just uses a state matrix to encode the intent over several seconds. We aim to avoid communication at every time of an entire intent trajectory, as this could overload the communication channel.

The remainder of this paper is structured as follows. In Section II, we develop the dynamic models of the predecessor-follower configuration and define the intent-based output regulation problem. In Section III, we present solutions to intent-based output regulation in a full information scenario and a partial information scenario. In Section IV, we design a

mechanism for each vehicle to autonomously construct its own intent. In Section V, we validate the proposed ideas with both synthetic and real-world data. In Section VI, we conclude the paper and discuss future research opportunities.

*Notation:* The following notation will be adopted: we use $x \in \mathcal{L}_2$ and $x \in \mathcal{L}_\infty$ to indicate that a vector-valued signal $x(\cdot) \in \mathbb{R}^n$ is bounded in the $\mathcal{L}_2$ and $\mathcal{L}_\infty$ norm. The $H_\infty$ norm of a stable transfer function $H(q)$ is defined by $\|H(q)\|_\infty := \sup_{w\geq 0} \sigma_{\max}(H(jw))$, where $q$ is the Laplace operator and $\sigma_{\max}(\cdot)$ is the maximum singular value.

## II. Problem Formulation

Let us consider two vehicles in predecessor-follower configuration, as depicted in Fig. 1(a). For each vehicle $i$, its longitudinal dynamics can be represented as

$$\begin{aligned} \dot{s}_i(t) &= v_i(t) \\ \dot{v}_i(t) &= a_i(t), \end{aligned} \tag{1}$$

where $s_i$, $v_i$, $a_i$ denote the longitudinal position, velocity, and acceleration of vehicle $i$. We model the engine/powertrain dynamics of each vehicle $i$ as in the literature [36]–[38]

$$\tau_i \dot{a}_i(t) = -a_i(t) + u_i(t), \tag{2}$$

where $u_i$ denotes the desired acceleration input provided via the vehicle pedals, and $\tau_i > 0$ is the time constant of vehicle $i$, representing the time necessary to reach a desired acceleration due to the engine/powertrain dynamics. After indexing the predecessor as vehicle $i+1$, we consider an inter-vehicle time-headway spacing error commonly adopted in the literature [39]

$$e_i(t) = s_{i+1}(t) - s_i(t) - h v_i(t) - r, \tag{3}$$

where $s_{i+1} - s_i$ is the relative distance between the two vehicles, $h$ is the time headway ($h > 0$ implies that the desired inter-vehicle spacing increases as the velocity increases), and $r > 0$ is a standstill safety distance which may include the vehicle length, so as to get the bumper-to-bumper distance. Let us further define the relative velocity as $\nu_i = v_{i+1} - v_i$. Then, the dynamics of the predecessor-follower system can be written as:

$$\begin{bmatrix} \dot{e}_i(t) \\ \dot{\nu}_i(t) \\ \dot{a}_i(t) \end{bmatrix} = \begin{bmatrix} 0 & 1 & -h \\ 0 & 0 & -1 \\ 0 & 0 & -\frac{1}{\tau_i} \end{bmatrix} \begin{bmatrix} e_i(t) \\ \nu_i(t) \\ a_i(t) \end{bmatrix} + \begin{bmatrix} 0 \\ 0 \\ \frac{1}{\tau_i} \end{bmatrix} u_i(t) + \begin{bmatrix} 0 \\ 1 \\ 0 \end{bmatrix} a_{i+1}(t), \tag{4}$$

with $x_i = \begin{bmatrix} e_i & \nu_i & a_i \end{bmatrix}^\top$ being the state vector of the predecessor-follower pair. In (4), $u_i$ is the control input of the follower vehicle to be designed, and $a_{i+1}$ is the acceleration of the predecessor vehicle acting as an exogenous disturbance to the predecessor-follower system. Note that the state components $e_i$, $\nu_i$, $a_i$ of the predecessor-follower pair can be measured by the follower vehicle with standard on-board sensors (radar, tachometer, accelerometer), commonly available on ACC-equipped or CACC-equipped vehicles. Such sensors cannot measure the predecessor acceleration $a_{i+1}$, which requires the predecessor vehicle to share it with its follower via wireless communication. In the rest of the work, we follow a continuous-time formulation to better align to the vast majority of CACC and output regulation literature. Nevertheless, the proposed ideas are amenable to digital implementation, as verified in the numerical validation part.

### A. Ideal status-sharing formulation

The control problem is how to design $u_i$: to introduce this control problem, let us consider the status-sharing[1] controller $u_i$ from the literature [40], [41]

$$u_i(t) = \theta_1 e_i(t) + \theta_2 \nu_i(t) + (1 - \tau h^{-1} - h\theta_2) a_i(t) + \tau h^{-1} a_{i+1}(t), \tag{5}$$

with arbitrary $\theta_1 > 0$, $\theta_2 > 0$. The literature has shown that (5) guarantees disturbance decoupling and string stability properties, defined as follows.

**Definition 1** (Status-sharing CACC)**.** *For the predecessor-follower system (4) with spacing policy (3), the status-sharing controller $u_i$ in (5) guarantees*

1) output regulation with disturbance decoupling*: for any bounded signal $a_{i+1}(\cdot)$, we have*

$$\lim_{t\to\infty} e_i(t) = 0. \tag{6}$$

2) string stability*: for any bounded signal $a_{i+1}(\cdot)$ and any $\Delta t > 0$, we have*

$$\int_t^{t+\Delta t} (a_i^2(\ell) - a_{i+1}^2(\ell)) d\ell \leq 0. \tag{7}$$

Disturbance decoupling CACC frameworks have been rigorously demonstrated in prior literature [42] to simultaneously accommodate heterogeneous parameters $\tau_i$ while maintaining formal collision avoidance guarantees. Thus, Definition 1 ensures a wide set of desirable properties for status-sharing CACC. The controller (5) is regarded as ideal because it relies on perfect wireless communication of $a_{i+1}(t)$ at each time $t$ (to be interpreted as the predecessor vehicle sharing its status with the follower). However, wireless communication is unreliable [10], [14], so that the ideal properties in Definition 1 would be lost during communication failures.

### B. Proposed intent-sharing formulation

Let us now introduce an 'intent' of the predecessor vehicle, shared to the follower vehicle through wireless communication in a similar way as the status. Such intent can be interpreted as the behavior of the predecessor vehicle in the near future: by this, even when the current status of the predecessor is unavailable during communication failures, the follower vehicle can still rely on the latest communicated intent to reconstruct the missing status and recover desirable properties, cf. Fig. 1(b). Inspired by the exosystem in output regulation [32], [43], the intent of the predecessor vehicle is taken as

$$\begin{aligned} \dot{w}_{i+1}(t) &= S w_{i+1}(t), \quad S = \begin{bmatrix} 0 & 1 & 0 \\ -\Omega^2 & 0 & 0 \\ 0 & 0 & 0 \end{bmatrix}, \\ a_{i+1}(t) &= H w_{i+1}(t), \quad H = \begin{bmatrix} 1 & 0 & 1 \end{bmatrix}, \end{aligned} \tag{8}$$

[1]We refer to (5) as status-sharing controller because it uses the current state of the predecessor-follower pair in (4) and the current acceleration of the predecessor vehicle.

where $w_{i+1}$ denotes the exosystem state (or intent state), so that $a_{i+1}$ is a linear combination of the intent state. To highlight the meaning of (8), recall that the solution to dynamics (8) is in the form $a_{i+1}(t) = \alpha \sin(\Omega t + \phi) + \beta$, where $\alpha$, $\phi$, $\beta$ are the amplitude, phase and bias depending on the initial condition $\omega_{i+1}(0)$. While more complex behaviors (e.g., multi-modal) can be considered, the behavior encoded in (8) works in practice (as verified in the numerical validation part) and is simple enough to present the control design in an easy way.

The intent sharing control problem can be formally stated as follows.

**Intent-sharing CACC Problem:** *For the predecessor-follower system (4) with spacing policy (3) and intent (8), design a controller $u_i$ that guarantees*

1) intent-sharing output regulation*: for any bounded signal $a_{i+1}(\cdot)$ solution to the intent dynamics (8), we have*
$$\lim_{t\to\infty} e_i(t) = 0. \tag{9}$$
2) intent-sharing string stability*: for any bounded signal $a_{i+1}(\cdot)$ solution to the intent dynamics (8), we have*
$$\int_t^{t+\Delta t} (a_i^2(\ell) - a_{i+1}^2(\ell))d\ell \leq 0. \tag{10}$$

The main difference between the Intent-sharing CACC Problem and the ideal properties in Definition 1 is that output regulation and string stability are not defined for arbitrary $a_{i+1}(\cdot)$, but only for a class of $a_{i+1}(\cdot)$ compatible with the intent of the predecessor vehicle, i.e., a solution to the dynamics (8). The next section provides an answer to the proposed intent-sharing formulation. Note that under reliable communication, $a_{i+1}(\cdot)$ would be available at all times. In this full information scenario, the intent-sharing controller reduces to the status-sharing controller through direct use of the measured signal, bypassing intent reconstruction. This recovery of the classical design under full information scenario is formally established in the next section.

## III. Proposed intent-sharing solution

The main idea of the intent-sharing control design is to replace the ideal controller (5) with

$$u_i(t) = \theta_1\hat{e}_i(t)+\theta_2\hat{\nu}_i(t)+(1-\tau_i h^{-1}-h\theta_2)\hat{a}_i(t)+\tau_i h^{-1}\hat{a}_{i+1}(t) \tag{11}$$

where the signals $\hat{e}_i$, $\hat{\nu}_i$, $\hat{a}_i$, $\hat{a}_{i+1}$ are reconstructed versions of the signals $e_i$, $\nu_i$, $a_i$, $a_{i+1}$ in (5). Note that (11) has the same structure as (5), with signals that have the same physical interpretation (spacing error, relative velocity, acceleration) as the signals in (5). Such a structure allows for a seamless integration of status sharing and intent sharing. The signals $\hat{e}_i$, $\hat{\nu}_i$, $\hat{a}_i$ will be reconstructed by an observer while on-board sensors measure the states $e_i$, $\nu_i$, $a_i$. The fact that the states remain available during communication failures, allows the observer to form a set of observation errors $e_i - \hat{e}_i$, $\nu_i - \hat{\nu}_i$, $a_i - \hat{a}_i$, used to reconstruct the exosystem state $\hat{w}_{i+1}$ and $\hat{a}_{i+1}$. Consequently, an observer-based control structure is adopted, in which the observed signals replace the actual signals in the control law. Closed-loop stability analysis will prove the convergence of the observation errors to zero.

### A. Full information intent-sharing scenario

Before introducing the main design of (5), we present the ideal case with full information, i.e., perfect communication. We show that the controller structure in (5) already embeds the intent, as formalized in the following result.

**Theorem 1** (Full information intent-sharing protocol)**.** *Consider the predecessor-follower system (4) with spacing policy (3) and intent (8). When all signals $e_i$, $\nu_i$, $a_i$, $a_{i+1}$ are available at time $t$, the same controller (5) used for status-sharing CACC also solves the intent-sharing CACC Problem.*

*Proof.* The main idea of the proof is to show that the controller (5) solves a regulation problem with the predecessor intent playing the role of an exosystem. To this purpose, let us compactly write the predecessor-follower system (4) as

$$\begin{aligned} \dot{x}_i &= Ax_i + Bu_i + Pw_{i+1} \\ e_i &= Cx_i, \end{aligned} \tag{12}$$

with matrices

$$\begin{aligned} A &= \begin{bmatrix} 0 & 1 & -h \\ 0 & 0 & -1 \\ 0 & 0 & -\frac{1}{\tau_i} \end{bmatrix}, \quad B = \begin{bmatrix} 0 \\ 0 \\ \frac{1}{\tau_i} \end{bmatrix}, \\ P &= \begin{bmatrix} 0 \\ 1 \\ 0 \end{bmatrix} \begin{bmatrix} 1 & 0 & 1 \end{bmatrix}, \quad C = \begin{bmatrix} 1 & 0 & 0 \end{bmatrix}. \end{aligned} \tag{13}$$

It is straightforward to show that $(A, B)$ is stabilizable. Because $S$ in (8) is antistable, we know from output regulation theory [31], [32], [44], [45] that output regulation is solvable if and only if the following linear matrix equations

$$\begin{aligned} \Pi S &= A\Pi + P + B\Gamma \\ 0 &= C\Pi, \end{aligned} \tag{14}$$

have a solution pair $(\Pi, \Gamma)$. Before finding such a solution, let us recall why (14) allows to solve an output regulation problem. Let $K$ be a matrix such that $A + BK$ is stable (such $K$ can always be found because $(A, B)$ is stabilizable). We now show that a controller in the form

$$u_i = K(x_i - \Pi w_{i+1}) + \Gamma w_{i+1}, \tag{15}$$

achieves output regulation. Substituting such controller in (12) gives the closed-loop system

$$\begin{aligned} \dot{x}_i &= (A + BK)x_i + (P - BK\Pi + B\Gamma)w_{i+1} \\ \dot{w}_{i+1} &= Sw_{i+1} \\ e_i &= Cx_i. \end{aligned} \tag{16}$$

Let us define the state transformation $\bar{x}_i = x_i - \Pi w_{i+1}$, whose dynamics are

$$\begin{aligned} \dot{\bar{x}}_i &= (A+BK)x_i+(P-BK\Pi+B\Gamma)w_{i+1}-\Pi S w_{i+1} \\ &= (A+BK)x_i - A\Pi w_{i+1} - BK\Pi w_{i+1} \\ &= A(x_i - \Pi w_{i+1}) + BK(x_i - \Pi w_{i+1}) \\ &= (A+BK)\bar{x}_i, \end{aligned} \tag{17}$$

where we have used the first of the linear matrix equations in (14). With a proper design of $K$, the matrix $A + BK$ can be

made stable, so that all the trajectories of (17) converge to the equilibrium $\bar{x}_i = 0$. Furthermore, we have

$$e_i = Cx_i - C\Pi w_{i+1} = C\bar{x}_i, \tag{18}$$

where we have used the second of the linear matrix equations in (14). We conclude that if the two linear matrix equations in (14) hold, then $e_i$ converges to zero.

As a next step, we choose $K$ so that the controller (15) boils down to the controller (5). Such a choice for $K$ is

$$K = \begin{bmatrix} \theta_1 & \theta_2 & 1 - \tau_i h^{-1} - h\theta_2 \end{bmatrix}, \tag{19}$$

leading to

$$\Gamma - K\Pi = \tau_i h^{-1} H = \begin{bmatrix} \tau_i h^{-1} & 0 & \tau_i h^{-1} \end{bmatrix}, \tag{20}$$

where we have used the fact that $u_i = K(x_i - \Pi w_{i+1}) + \Gamma w_{i+1}$ is equivalently written as

$$\begin{aligned} u_i &= \begin{bmatrix} \theta_1 & \theta_2 & 1 - \tau_i h^{-1} - h\theta_2 \end{bmatrix} x_i + \tau_i h^{-1} \begin{bmatrix} 1 & 0 & 1 \end{bmatrix} w_{i+1} \\ &= Kx_i + Ew_{i+1}, \end{aligned} \tag{21}$$

with $E = \Gamma - K\Pi$. Next, let us calculate a solution $(\Pi, \Gamma)$ to (14) for the predecessor-follower system (4). Decompose the solution as

$$\Pi = \begin{bmatrix} \pi_{11} & \pi_{12} & \pi_{13} \\ \pi_{21} & \pi_{22} & \pi_{23} \\ \pi_{31} & \pi_{32} & \pi_{33} \end{bmatrix}, \quad \Gamma = \begin{bmatrix} \gamma_1 & \gamma_2 & \gamma_3 \end{bmatrix}. \tag{22}$$

From $C\Pi = 0$, we can derive the following

$$\begin{bmatrix} \pi_{11} & \pi_{12} & \pi_{13} \end{bmatrix} = 0.$$

Meanwhile, from $\Pi S = A\Pi + B\Gamma + P$, we can get

$$A\Pi + B\Gamma + P = \begin{bmatrix} \pi_{21} - h\pi_{31} & \pi_{22} - h\pi_{32} & \pi_{23} - h\pi_{33} \\ 1 - \pi_{31} & -\pi_{32} & 1 - \pi_{33} \\ \frac{\gamma_1 - \pi_{31}}{\tau} & \frac{\gamma_2 - \Pi_{32}}{\tau} & \frac{\gamma_3 - \pi_{33}}{\tau} \end{bmatrix}$$

$$\begin{bmatrix} 0 & 0 & 0 \\ -\Omega^2\pi_{22} & \pi_{21} & 0 \\ -\Omega^2\pi_{32} & \pi_{31} & 0 \end{bmatrix} = \begin{bmatrix} \pi_{21} - h\pi_{31} & \pi_{22} - h\pi_{32} & \pi_{23} - h\pi_{33} \\ 1 - \pi_{31} & -\pi_{32} & 1 - \pi_{33} \\ \frac{\gamma_1 - \pi_{31}}{\tau} & \frac{\gamma_2 - \pi_{32}}{\tau} & \frac{\gamma_3 - \pi_{33}}{\tau} \end{bmatrix}.$$

Hence, the solution $(\Pi, \Gamma)$ to (14) exists and takes the form

$$\Pi = \begin{bmatrix} 0 & 0 & 0 \\ \frac{h\gamma_2}{\tau - h} & \frac{-h^2\gamma_2}{\tau - h} & h \\ \frac{\gamma_2}{\tau - h} & \frac{-h\gamma_2}{\tau - h} & 1 \end{bmatrix}, \quad \Gamma = \begin{bmatrix} \gamma_1 & \gamma_2 & 1 \end{bmatrix}, \tag{23}$$

with

$$\gamma_1 = \frac{\Omega^2 h\tau + 1}{\Omega^2 h^2 + 1}, \quad \gamma_2 = \frac{\tau - h}{\Omega^2 h^2 + 1}. \tag{24}$$

To show string stability in the sense of (10), we calculate the transfer function from $a_{i+1}$ to $a_i$ of the closed loop formed by (12) and (15). Since $a_i = \tilde{C}x_i$, with $\tilde{C} = \begin{bmatrix} 0 & 0 & 1 \end{bmatrix}$, the transfer function from $a_{i+1}$ to $a_i$ is given by

$$G(q) = \tilde{C}(qI - A - BK)^{-1}\left(B\tau_i h^{-1} + \begin{bmatrix} 0 \\ 1 \\ 0 \end{bmatrix}\right) = \frac{1}{hq + 1}, \tag{25}$$

where $q$ is the Laplace operator. Let $q = j\omega$ and calculate the magnitude of the transfer function

$$|G(j\omega)| = \sqrt{\frac{1}{(h\omega)^2 + 1}} \leq 1, \quad \forall \omega \geq 0. \tag{26}$$

The $\mathcal{H}_\infty$ norm of $G$ is $\|G\|_\infty = \max_{\omega \geq 0} |G(j\omega)| = 1$. Because the $\mathcal{H}_\infty$ norm of the system is equivalent to its induced $\mathcal{L}_2$ gain, we have

$$\inf_{\Delta t > 0} \int_t^{t + \Delta t} (\|G\|_\infty^2 (a_{i+1}^2(\ell) - a_i^2(\ell))) d\ell \leq 0, \tag{27}$$

implying that condition (10) holds for any $h > 0$. This concludes the proof. □

**Remark 1.** *Theorem 1 implies that the same CACC protocol used in a status sharing situation (with communication of the current $a_{i+1}$ only) is also valid for an intent sharing situation. This means that, as long as communication of the current $a_{i+1}$ is possible, there is* no *additional benefit in communicating extra intent variables.*

### *B. Partial information intent-sharing scenario*

We now further look at the partial information scenario, i.e., with information not fully available due to communication failures. The following result shows that if $a_{i+1}$ is missing, it can be reconstructed as a properly designed $\hat{a}_{i+1}$.

**Theorem 2** (Partial information intent-sharing protocol)**.** *Consider the predecessor-follower system (4) with spacing policy (3) and intent (8). The controller*

$$u_i = K\hat{x}_i + E\hat{w}_{i+1} \tag{28}$$

*with $K$, $E$ as in (19)-(21), along with the state estimator and exosystem estimator*

$$\begin{aligned} \dot{\hat{x}}_i &= A\hat{x}_i + P\hat{w}_{i+1} + L_1(C\hat{x}_i - e_i) + Bu_i \\ \dot{\hat{w}}_{i+1} &= S\hat{w}_{i+1} + L_2(C\hat{x}_i - e_i) \end{aligned} \tag{29}$$

*with $A$, $B$, $C$, $P$ as in (12)-(13), and $L_1$, $L_2$ observer gains (cf. their design after* (32)*), solves the intent-sharing CACC Problem. With $\hat{x}_i = \begin{bmatrix} \hat{e}_i & \hat{\nu}_i & \hat{a}_i \end{bmatrix}$, the controller (28) can be equivalently written in the form (11), where the reconstructed version of $a_{i+1}$ is obtained as*

$$\hat{a}_{i+1} = H\hat{w}_{i+1}. \tag{30}$$

*Proof.* In line with the proof of Theorem 1, the goal is to show that $e_i$ converges to zero. To this purpose, let us define the system state observation error $\tilde{x}_i := \hat{x}_i - x_i$ and the exosystem state observation error $\tilde{w}_{i+1} := \hat{w}_{i+1} - w_{i+1}$. Then, we rewrite the closed-loop system formed by (4) and (29) as

$$\begin{aligned} \dot{x}_i = (A + BK)x_i + Pw_{i+1} - BK\Pi w_{i+1} \\ + B\Gamma w_{i+1} + BK\tilde{x}_i + B(\Gamma - K\Pi)\tilde{w}_{i+1} \end{aligned} \tag{31}$$

leading to the observation error dynamics

$$\begin{bmatrix} \dot{\tilde{x}}_i \\ \dot{\tilde{w}}_{i+1} \end{bmatrix} = \begin{bmatrix} A + L_1 C & P \\ L_2 C & S \end{bmatrix} \begin{bmatrix} \tilde{x}_i \\ \tilde{w}_{i+1} \end{bmatrix}, \tag{32}$$

Because the pair $(A, C)$ is detectable, an observer gain $L_1$ can always be found such that $A + L_1 C$ is stable. Analogously,

along standard reasoning for observer design, an observer gain $L_2$ can always be found such that the state matrix of the observation error dynamics in (32) is stable [32]. This implies that the errors $x_{i+1}-\hat{x}_{i+1}$ and $w_{i+1}-\hat{w}_{i+1}$ converge to zero. As a result, the controller (11) using feedback from $\hat{x}_{i+1}$ and $\hat{w}_{i+1}$ will converge to the controller (28) using feedback from $x_{i+1}$ and $w_{i+1}$, that is, the following convergence holds

$$\begin{aligned}\theta_1\hat{e}_i(t)+\theta_2\hat{\nu}_i(t)+(1-\tau_i h^{-1}-h\theta_2)\hat{a}_i(t)+\tau_i h^{-1}\hat{a}_{i+1}(t)\rightarrow\\ \theta_1 e_i(t)+\theta_2\nu_i(t)+(1-\tau_i h^{-1}-h\theta_2)a_i(t)+\tau_i h^{-1}a_{i+1}(t).\end{aligned} \tag{33}$$

Thus, a similar reasoning as in the proof of Theorem 1 applies, meaning that the output $e_i$ is regulated to zero asymptotically for any signal $a_{i+1}(\cdot)$ compatible with the intent (8). □

Thanks to (33), the partial information design achieves the same steady-state behavior as the full information design and thereby inherits its desirable properties including string stability. Such steady-state analysis is consistent with the standard treatment of string stability in CACC, as transfer function methods inherently characterize system behavior under steady-state conditions [7]. To the best of the authors' knowledge, transient analysis of CACC properties remains largely unexplored and represents a promising direction for future research.

**Remark 2.** *Theorem 2 implies that $a_{i+1}-\hat{a}_{i+1}$ converge to zero under the intent condition (8), i.e., $a_{i+1}$ can be reconstructed as $\hat{a}_{i+1}$ even during communication failures. We emphasize that the controller (28)-(29) operates exclusively using on-board sensors, without inter-vehicle communication.*

The controller (28)-(29) relies on the availability of $S$, encoding the intent of the predecessor vehicle. The final step is to allow the predecessor to internally construct its own intent in the form (8). This is achieved using a suitable estimator.

## IV. Generation of the Exosystem

The predecessor vehicle can autonomously generate its intent model in real-time through online processing, as demonstrated by the following results.

**Theorem 3.** *Consider the predecessor vehicle model*

$$\begin{aligned}\dot{s}_{i+1}(t)&=v_{i+1}(t)\\ \dot{v}_{i+1}(t)&=a_{i+1}(t)=Hw_{i+1}(t),\end{aligned} \tag{34}$$

*where $w_{i+1}(t)$ obeys the intent $\dot{w}_{i+1}(t)=S^*w_{i+1}(t)$ with*

$$S^*=\begin{bmatrix}0&1&0\\-\Omega^{*2}&0&0\\0&0&0\end{bmatrix}, \tag{35}$$

*but the intent state matrix $S^*$ is a priori unknown to the predecessor vehicle. The predecessor vehicle can generate an estimate $S(t)$ of $S^*$, namely*

$$S(t)=\begin{bmatrix}0&1&0\\-\Omega^{2}(t)&0&0\\0&0&0\end{bmatrix}, \tag{36}$$

*from on-board measurements of $a_{i+1}$, using the estimator*

$$\begin{aligned}\dot{\Theta}(t)&=F\varepsilon(t)\Phi(t),\\ \varepsilon(t)&=\frac{z(t)-\hat{z}(t)}{m_s^2(t)}=\frac{z(t)-\Theta^\top(t)\Phi(t)}{m_s^2(t)},\end{aligned} \tag{37}$$

*where $F=F^\top>0$ is an adaptive gain, $m_s^2(t)=1+\Phi^\top(t)\Phi(t)$ is a normalizing signal, and*

$$\begin{aligned}\Theta(t)&=\begin{bmatrix}-\Omega^2(t)&\hat{w}_3(t)\Omega^2(t)\end{bmatrix}\\ \Phi(t)&=\begin{bmatrix}\frac{\lambda_0}{q^2+\lambda_1 q+\lambda_0}a_{i+1}(t)\\ \frac{\lambda_0}{q^2+\lambda_1 q+\lambda_0}\end{bmatrix}\\ z(t)&=\frac{\lambda_0 q^2}{q^2+\lambda_1 q+\lambda_0}a_{i+1}(t),\end{aligned} \tag{38}$$

*with $\lambda_0,\lambda_1>0$. Then, the estimator (37) guarantees that $S(t)$ converges to $S^*$ exponentially, i.e., the estimated intent converges to a priori unknown intent of the predecessor.*

*Proof.* Refer to the Appendix. □

**Remark 3.** *Theorem 3 allows the predecessor vehicle to generate its own intent model from on-board measurements ($\Phi$ and $z$ in (38) are available to vehicle $i+1$ from on-board sensing of $a_{i+1}$). Such generation can be performed by the predecessor vehicle online, regardless of the communication status between the predecessor and the follower vehicle. When communication is available, the generated intent can be readily communicated to the follower; when communication fails, the follower vehicle can use the latest communicated intent to reconstruct the missing status of the predecessor in the near future, in accordance with the result of Theorem 2.*

Exponential convergence of $S(t)$ to $S^*$ makes the properties in Theorem 1 and Theorem 2 be attained exponentially fast at steady state. We emphasize that, instead of communicating the entire matrix $S(t)$, a lighter communication approach is that the predecessor communicates only the scalar $\Omega(t)$, letting the follower construct $S(t)$ using (36).

## V. Validation Studies

We validate the proposed theory using synthetic and real-world scenarios. To simulate unreliability of the wireless channel, we consider V2V communication to be initially available, followed by a period where communication fails for a few seconds, and finally normal V2V communication is restored. To validate the fact that the proposed exosystem model can encode the intent over several seconds, we consider communication failures up to 6 seconds. To the purpose of comparisons, we consider two state-of-the-art ways to deal with communication failures [13], [14]:

i) *Switch to ACC*: when communication fails, the follower vehicle will switch from CACC to ACC, by only using on-board sensing without any $a_{i+1}$. In view of (5), this is equivalent to assuming that the predecessor vehicle keeps zero $a_{i+1}$ until communication is restored.

ii) *Constant intent*: when communication fails, the follower vehicle will use the latest communicated status $a_{i+1}$ in the CACC protocol. This is equivalent to assuming that

the predecessor vehicle constantly keeps the last communicated status $a_{i+1}$ until communication is restored.

To numerically compare the performance, two types of energy (for spacing error and for follower acceleration) are calculated and used as performance indicators.

*Energy of spacing error in the time interval* $[t_1, t_2]$*:*

$$\int_{t_1}^{t_2} e_i^2(\ell)\mathrm{d}\ell \tag{39}$$

*Energy of follower acceleration in the time interval* $[t_1, t_2]$*:*

$$\int_{t_1}^{t_2} a_i^2(\ell)\mathrm{d}\ell \tag{40}$$

where the interval $[t_1, t_2]$ is taken as the period when communication fails. The rationale is the following. The energy of the spacing error measures the capability of the protocol to stick to the desired inter-vehicle spacing: it is desirable for the spacing error to have low energy. The energy of the follower acceleration measures the capability of the protocol to avoid amplification of the energy of the predecessor acceleration: it is desirable for the follower acceleration to have low energy in order to damp the energy of the predecessor acceleration.

Based on the above performance indicators, we validate the different implementations of CACC on both synthetic and real-world data, as explained hereafter. The integrals (39)-(40) are formulated in continuous time for consistency with the formulation we adopted. Nevertheless, the numerical implementation of all protocols is digital.

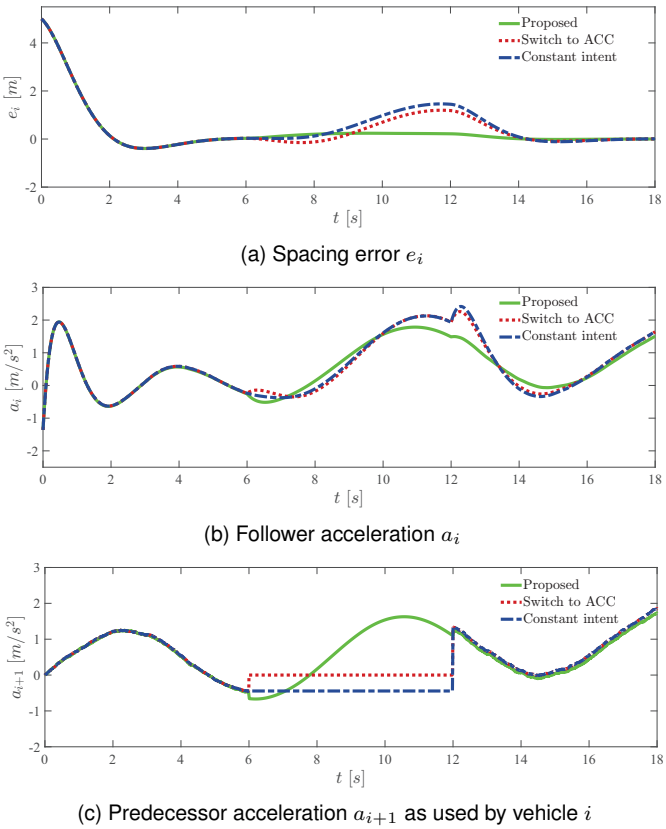


(a) Spacing error $e_i$

(b) Follower acceleration $a_i$

(c) Predecessor acceleration $a_{i+1}$ as used by vehicle $i$

Fig. 2: Comparative experiments with synthetic data.

### A. Validation with synthetic data

In this validation scenario, the acceleration of the predecessor vehicle is defined as a multi-modal sine wave $a_{i+1}(t) = \sin(\Omega_1 t) + \sin(\Omega_2 t)$ with $\Omega_1 = 0.75, \Omega_2 = 0.1$. The meaning of such a multi-modal form is to include both a slowly time-varying and a faster time-varying intent. One may regard the slowly time-varying intent as described by a slowly time-varying bias $\beta$, and the faster time-varying intent as described by $\Omega$ in the exosystem model (8). As such, the multi-modal sine wave is more general than the behavior in the theoretical analysis, and can be used to validate the effectiveness of the proposed method beyond the hypotheses made for stability analysis. To further relax the theoretical hypotheses and obtain a more naturalistic behavior, we have also included Brownian noise in the communication channel.

As it can be seen from the results in Fig. 2 and Table I, the proposed intent-sharing implementation outperforms the other comparative methods, especially in terms of energy of the spacing error. A large energy of the spacing error means that the follower vehicle would largely deviate from the desired inter-vehicle distance. For example, if the spacing error is positive and far from zero, the follower vehicle is losing cohesiveness with the predecessor; if the spacing error is negative and far from zero, it indicates that the follower vehicle is approaching the predecessor too much, leading to possible rear-end collision. The small energy of the spacing error in Table I validates the capability of the proposed protocol to stick to the desired inter-vehicle distance even during communication loss.

TABLE I: Energy of spacing error and of follower acceleration with synthetic data, during communication loss period

| | $\int e_i^2 d\ell$ | $\int a_i^2 d\ell$ |
|---|---|---|
| Proposed | **0.28** | **9.97** |
| Switch to ACC | 3.53 | 13.78 |
| Constant intent | 5.73 | 14.52 |

### B. Robustness to different parameters

Reliability and low latency of the communication channel are critical requirements for Intelligent Transportation Systems, refer to [46] for a comprehensive review on communication in vehicular networks. This and other studies quantify a maximum of 100 ms latency for safety services, which can be extended to 500 ms for non-safety services [47]–[49].

In a CACC scenario, safety is crucial: when the communication conditions exceed the maximum latency, it is expected that the protocol activates some resilience mechanism. In this validation scenario, we aim to show the robustness to different loss periods of the proposed implementation of intent sharing. As illustrated by Figure 3 and Table II, the proposed approach is robust across all the tested intervals, as the performance indicators remain close to the ideal communication ($\Delta t_{\text{fail}} = 0$ s). Let us mention that, in order to have a fair comparison across all intervals, the performance indexes are calculated over the

TABLE II: Energy of spacing error and of follower acceleration with synthetic data, for different duration of the communication loss

| $\Delta t_{\text{fail}}$ | 0s | 1s | 2s | 3s | 4s | 5s | 6s |
|---|---|---|---|---|---|---|---|
| $\int e_i^2 d\ell$ | 0 | 0.03 | 0.07 | 0.13 | 0.18 | 0.23 | 0.28 |
| $\int a_i^2 d\ell$ | 9.47 | 9.74 | 9.43 | 9.63 | 9.86 | 9.99 | 9.97 |

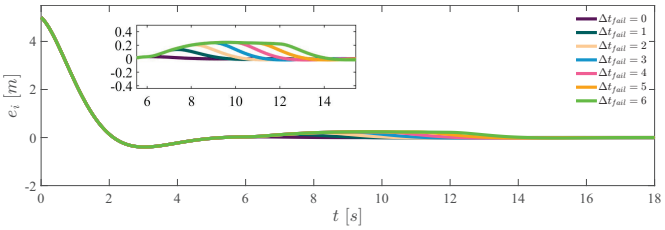


(a) Spacing error $e_i$

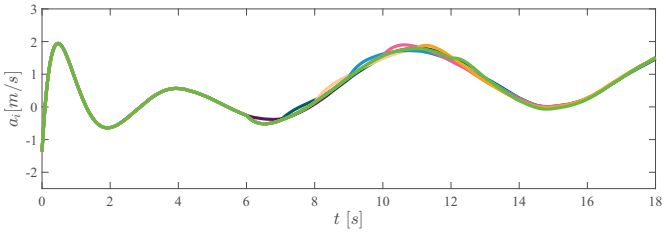


(b) Follower acceleration $a_i$

Fig. 3: Comparisons with different duration of the communication loss.

same integration interval, corresponding to the scenario with longest communication loss ($\Delta t_{\text{fail}} = 6$ s).

This validation scenario supports the fact that the exosystem matrix used to describe the intent can encode the behavior of the predecessor vehicle over several seconds of communication failure. Indeed, in the tests of Figure 3 and Table II, communication is lost at the same time instant, meaning that the same exosystem matrix (received by the follower vehicle before the communication is lost) can be used for up to 6 $s$ without evident performance loss.

To show the robustness of the proposed approach to the choice of the observer gain, refer to the results in Fig. 4. In order to have a systematic way to design the gains, we make use of the Riccati equation for optimal filtering, applied to system (32),which yields two tunable weights, $Q$ and $R$, representing the noise covariance. In Fig. 4, we fix $Q$ and vary $R = 10^{-2}/\gamma$ according to $\gamma \in \{0.5, 1, 5, 10\}$. As expected from the proof of Theorem 2, the choice of the observer gain only affects the initial transient: after that, convergence to the same steady state behavior is observed. Note that the observer dynamics (29) can run independently of whether communication is active or not: this allows the

TABLE III: Energy of spacing error and of follower acceleration with real-world highD data, during communication loss period

| | $\int e_i^2 d\ell$ | $\int a_i^2 d\ell$ |
|---|---|---|
| Proposed | **1.42** | **20.61** |
| Switch to ACC | 5.21 | 21.10 |
| Constant intent | 3.44 | 20.70 |

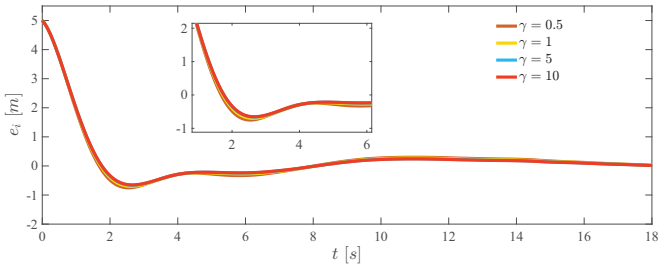


Fig. 4: Spacing error performance under different LQR gain settings.

dynamics to converge to their steady-state behavior even when communication is active.

### C. Validation with real-world data

In this validation scenario, the vehicle data for the predecessor vehicle (position, velocity, acceleration) are obtained from the publicly available highD dataset [50]. The highD dataset is a dataset of naturalistic vehicle trajectories recorded on German highways, as shown in Fig. 5. The main advantage of highD data is to exhibit more realistic behavior and more realistic measurement noise as compared to idealized synthetic data. On the other hand, because the highD dataset was recorded using a camera-equipped drone, the limited field of view of the camera limits the length of the trajectories and their time-varying behavior. For this reason, synthetic data and real-world data are complementary and provide a holistic validation of the proposed protocol. The acceleration of the predecessor vehicle in the trajectories of the highD dataset is fitted via online estimation along the scheme in Theorem 3, so as to estimate online the corresponding $\Omega$ used in the intent model.

Fig. 6 presents the results for one of the trajectories extracted from the highD dataset, where the capability of the proposed protocol in keeping the spacing error small during communication failure is confirmed. We remind that, before communication failure occurs, all tested strategies behave in the same way because they make use of the same protocol: what changes is the protocol used during communication failure. Note that both Fig. 2 and Fig. 6 show that the two strategies used for comparisons (switch to ACC and constant intent) exhibit a ripple in the follower acceleration after communication is recovered: this ripple is caused by the discontinuity in predecessor acceleration at the time instant when communication is recovered. The proposed intent-sharing protocol does not exhibit such ripple, which validates the seamless integration between status sharing and intent sharing. Table III collects the average performance for several trajectories extracted from highD dataset, confirming that the proposed intent sharing implementation outperforms the


Fig. 5: Example scenario in highD dataset

comparative methods both in terms of energy of the spacing error and energy of the follower acceleration.

### D. Calculation of communication overhead

From a communication point of view, encoding the intent of a vehicle in the form of an exosystem state matrix is much lighter than encoding it as a predicted trajectory. To explain this point, let us assume that status sharing of $a_{i+1}$ is part of the nominal 25 Mbps bit rate and 10 Hz frequency reported for the most common communication protocols for CAVs (IEEE 802.11p and C-V2X protocols [51], [52]). Meanwhile:

- If the intent of a vehicle is encoded in the form of a predicted trajectory, one would need to communicate $a_{i+1}$ for a prediction horizon. A prediction horizon of, let us say, 1 second would require to communicate 10 future values of $a_{i+1}$, resulting in a communication rate potentially up to ten times larger (250 Mbps) as compared to status sharing.
- However, if the intent of a vehicle is encoded in the form of an exosystem state matrix as we propose, communication of the intent simply requires communication of the current $\Omega$, meaning that intent sharing would require at most double rate (50 Mbps) as compared to status sharing.

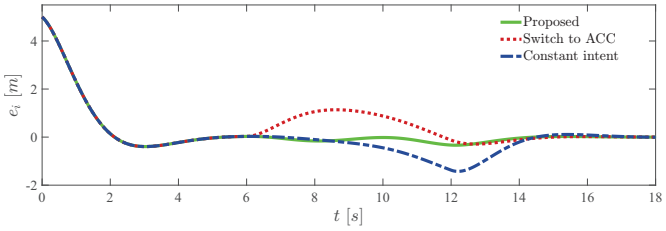


(a) Spacing error $e_i$

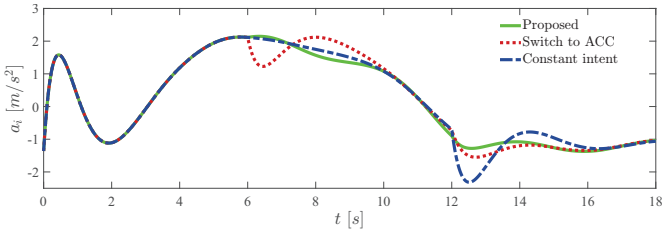


(b) Follower acceleration $a_i$

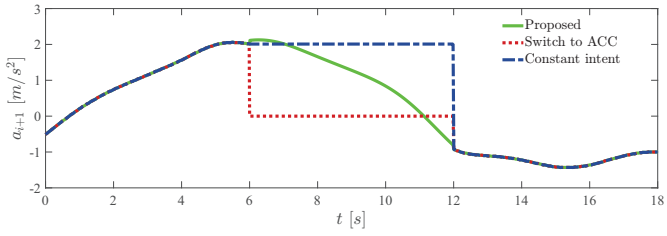


(c) Predecessor acceleration $a_{i+1}$ as used by vehicle $i$

Fig. 6: Comparative experiments with real-world highD data.

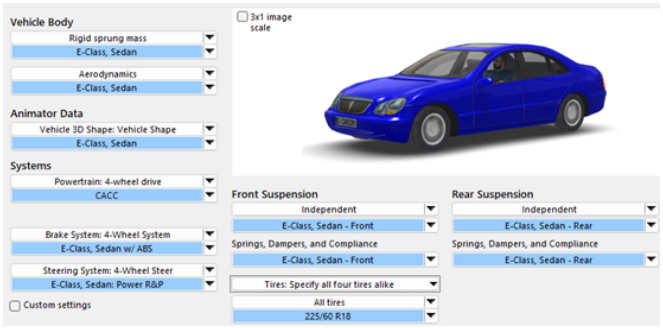


Fig. 7: Vehicle E-class configuration in CarSim.

Fig. 8: Initial configuration of the predecessor-follower system.

As the reported maximum data rate for IEEE 802.11p and C-V2X protocols is around 1 Gbps, a trajectory-based implementation of intent sharing would more easily congest the communication channel. Meanwhile, considering that the exosystem was shown able to encode the intent of a vehicle over a few seconds, the proposed implementation of intent sharing would be lighter in terms of communication overhead.

### E. Further validation with CarSim

In this validation scenario, the vehicle dynamics for both the predecessor and the follower vehicle are simulated with

TABLE IV: Energy of spacing error and of follower acceleration in CarSim for smooth and abrupt profiles, during communication loss period

| | Smooth profile | | Abrupt profile | |
|---|---|---|---|---|
| | $\int e_i^2 d\ell$ | $\int a_i^2 d\ell$ | $\int e_i^2 d\ell$ | $\int a_i^2 d\ell$ |
| Proposed | **0.27** | **10.79** | **1.46** | **37.83** |
| Switched to ACC | 3.34 | 13.34 | 7.92 | 40.23 |
| Constant intent | 5.40 | 14.05 | 60.70 | 53.53 |

the aid of CarSim. CarSim is software that can simulate and animate dynamic tests for cars using mathematical models based on 30+ years of research in vehicle dynamics. Fig. 7 and Fig. 8 show the E-class used to simulate the predecessor and the follower vehicle in the CarSim software, as well as the vehicle-following scenario on a straight road. Using CarSim, we can simulate braking, acceleration, and vehicle stability dynamics with high fidelity, thereby testing the applicability of our CACC implementation especially in the presence of ummodeled vehicle dynamics. We consider a smooth acceleration profile and an abrupt acceleration profile with two events of emergency braking.

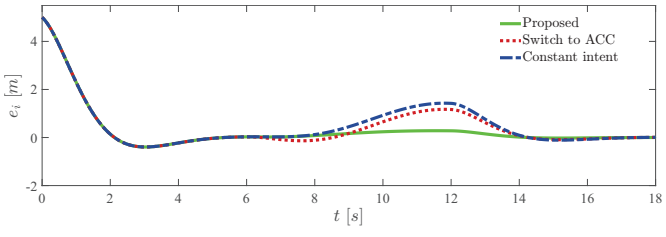


(a) Spacing error $e_i$

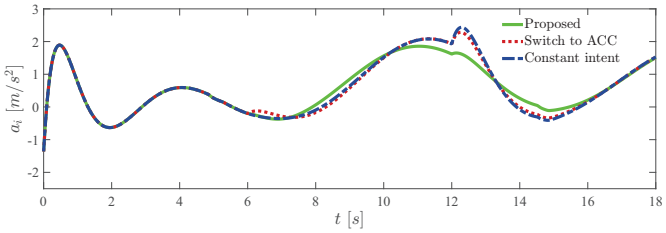


(b) Follower acceleration $a_i$

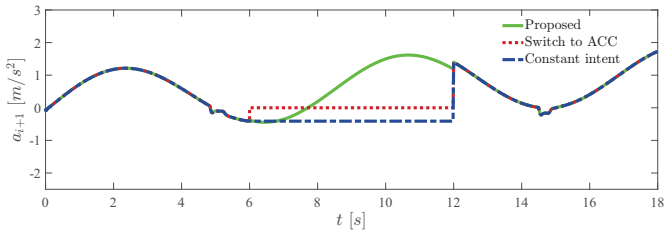


(c) Predecessor acceleration $a_{i+1}$ as used by vehicle $i$

Fig. 9: CarSim-based comparative experiments.

For the smooth profile, the left side of Table IV and Fig. 9 illustrate that, despite the more complex CarSim vehicle dynamics going beyond linear engine/powertrain dynamics, the proposed strategy keeps behaving consistently with the previous results, and continues to outperform the strategies based on switching to ACC and based on constant intent. This confirms some robustness of the proposed framework to modeling errors. Let us mention that Fig. 9(c) (similar consideration holds for Fig. 2(c) and Fig. 6(c)) do not report the actual predecessor acceleration $a_{i+1}$, but the predecessor acceleration used by vehicle $i$ in its own platooning strategy.

The abrupt profile with two events of emergency braking allows to further assess the robustness to modeling errors: in fact, the previous scenarios including the real-world highD dataset do not capture severe driving conditions. Evaluating performance under such safety-critical scenarios is essential

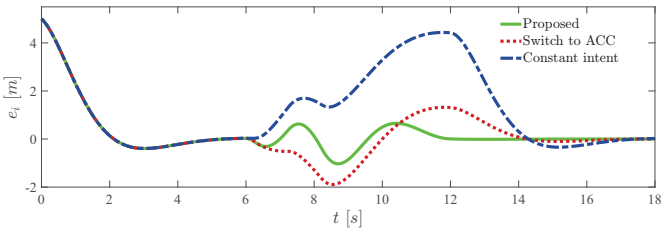


(a) Spacing error $e_i$

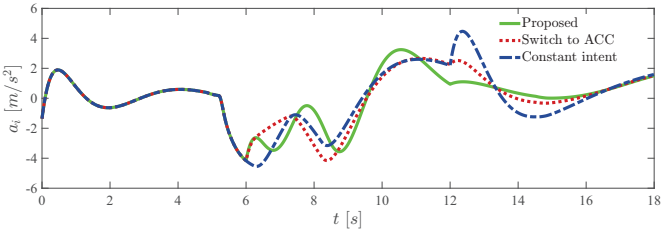


(b) Follower acceleration $a_i$

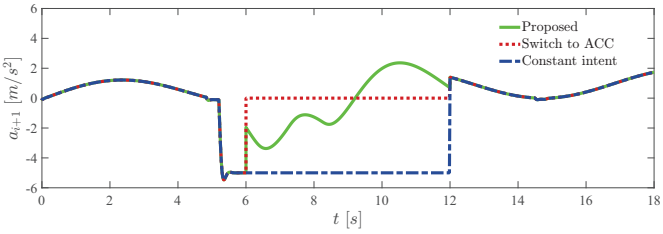


(c) Predecessor acceleration $a_{i+1}$ as used by vehicle $i$

Fig. 10: CarSim-based emergency braking comparative experiments.

for safety assessment. The two events of emergency braking occur in the intervals 5.2–6.2 s and 7.2–8.2 s. Note that the first emergency braking starts during the active communication period, but ends during the communication loss period. Meanwhile, the second emergency braking is fully during the communication loss period. As shown in the right side of Table IV and Fig. 10, maintaining the last received predecessor acceleration during communication failures leads to significantly higher energy in both spacing error and acceleration. The constant intent approach fails to account for driving transitions, such as the recovery phase following emergency braking. For a similar reason, switching to ACC and assuming zero acceleration for the follower vehicle may also make its estimated behavior become progressively inaccurate. In contrast, the proposed method achieves the lowest energy levels in both criteria. Although no method can receive information of the second braking during communication loss, the proposed method is better able to capture the recovery phase, even in the absence of V2V communication updates of the intent.

## VI. Conclusions and Future Work

In the context of Cooperative Adaptive Cruise Control (CACC), this work has provided a system-theoretic implementation of intent sharing in the perspective of output regulation. We presented analytical results showing two fundamental aspects of intent sharing: first, when vehicle-to-vehicle communication is reliable, intent sharing provides no benefit over

status sharing, as both paradigms result in the same protocol; second, intent sharing becomes advantageous when vehicle-to-vehicle communication is unreliable, in which case the latest communicated intent can be used to reconstruct the missing vehicle information in the near future. Along with theoretical analysis, numerical validations with both synthetic and real-world data have been given, where the benefits of CACC based on the proposed implementation of intent sharing have been shown against several state-of-the-art CACC protocols.

The results of this work provide several insights for future research directions. For example, it is of interest to consider more complex communication topologies, such as $k$-nearest-neighbors communication [53]. However, because on-board radar sensing can only be adopted between adjacent vehicles, non-adjacent neighbors would necessarily require to communicate not only acceleration, but also velocity and position, which would increase the communication overhead. Indeed, balancing between performance due to intent information and channel constraints due to communication overhead is another interesting venue for future research. Extensions of interest may include optimal design of the observers to handle modeling errors, discontinuous adaptation mechanisms to handle abrupt intent changes, and methods to guarantee transient performance [54]–[56].

## APPENDIX
## PROOF OF THEOREM 3

The proof is organized into three parts: in the first part, we provide the parametric model useful for estimation; in the second part we prove boundedness of the estimate; in the third part we prove convergence of the estimation error.

1) *Parametric model:* Due to the intent (35), it is straightforward to obtain that the following dynamics hold (here and in the following, let us omit time dependence whenever obvious)

$$\begin{aligned} a_{i+1} &= w_1 + w_3 \\ \ddot{w}_1 &= -\Omega^{*2} w_1,\ \dot{w}_3 = 0 \end{aligned} \tag{41}$$

where $w_1$ and $w_3$ indicate the first and third component of $w_{i+1} = \begin{bmatrix} w_1 & w_2 & w_3 \end{bmatrix}$. From (41), and applying a second-order stable filter, we get the parametric model

$$\ddot{a}_{i+1} = -\Omega^{*2}(a_{i+1} - w_3) \tag{42}$$

$$\begin{aligned} \frac{\lambda_0 q^2}{q^2+\lambda_1 q+\lambda_0} a_{i+1} &= \frac{-\Omega^{*2}\lambda_0}{q^2+\lambda_1 q+\lambda_0} a_{i+1} + \frac{w_3\Omega^{*2}\lambda_0}{q^2+\lambda_1 q+\lambda_0} \\ &= \begin{bmatrix} -\Omega^{*2} & w_3\Omega^{*2} \end{bmatrix} \begin{bmatrix} \frac{\lambda_0}{q^2+\lambda_1 q+\lambda_0} a_{i+1} \\ \frac{\lambda_0}{q^2+\lambda_1 q+\lambda_0} \end{bmatrix}. \end{aligned}$$

The parametric model is in the form $z = \Theta^{*\top}\Phi$ with

$$\Theta^* = \begin{bmatrix} -\Omega^{*2} & w_3\Omega^{*2} \end{bmatrix} \tag{43}$$

and $z$, $\Phi$ as in (38).

2) *Boundedness:* Define the parameter error $\tilde{\Theta} = \Theta - \Theta^*$ and consider the Lyapunov-like function

$$V(\tilde{\Theta}) = \frac{\tilde{\Theta}^\top F^{-1}\tilde{\Theta}}{2}. \tag{44}$$

Using the dynamics of the parameter error

$$\dot{\tilde{\Theta}} = F\frac{z-\hat{z}}{m_s^2}\Phi = -\frac{F\Phi\Phi^\top\tilde{\Theta}}{1+\Phi^\top\Phi}, \tag{45}$$

we can calculate the Lyapunov time derivative (44) along the solution of (45), resulting in

$$\dot{V} = \tilde{\Theta}^\top\Phi\varepsilon = -\varepsilon^2 m_s^2 \le 0, \tag{46}$$

where the second equality is obtained by substituting $\tilde{\Theta}^\top\Phi = -\varepsilon$ from (37). Since $V > 0$ and $\dot{V} \le 0$, it follows that $V(t)$ has a limit, i.e.,

$$\lim_{t\to\infty} V(\tilde{\Theta}(t)) = V_\infty < \infty. \tag{47}$$

The fact that $V, \tilde{\Theta} \in \mathcal{L}_\infty$, together with (37), imply that $\varepsilon, \varepsilon m_s \in \mathcal{L}_\infty$. In addition, it follows from (46) that

$$\int_0^\infty \varepsilon^2 m_s^2 \mathrm{d}\ell \le V(\tilde{\Theta}(0)) - V_\infty, \tag{48}$$

from which we establish that $\varepsilon m_s \in \mathcal{L}_2$ and hence $\varepsilon \in \mathcal{L}_2$. From (44), we have

$$|\dot{\tilde{\Theta}}| = |\dot{\Theta}| \le \|F\||\varepsilon m_s|\frac{|\Phi|}{m_s}, \tag{49}$$

which, together with $\frac{|\Phi|}{m_s} \in \mathcal{L}_\infty$ and $|\varepsilon m_s| \in \mathcal{L}_2$, imply that $\dot{\Theta} \in \mathcal{L}_2 \bigcap \mathcal{L}_\infty$. Thus, boundedness of all signals of interest has been derived.

3) *Convergence:* The dynamics of $a_{i+1}$ derived in (41) shows that the acceleration of the predecessor vehicle contains a sinusoidal signal with bias, thus providing persistence of excitation for the estimation of the two components of $\Theta^*$ [57], [58]. Namely, for a bounded $a_{i+1}$, we have that $\Phi, m_s$ are bounded and

$$\int_t^{t+T_0} \frac{\Phi\Phi^\top}{m_s^2}\mathrm{d}\tau \ge \frac{1}{m_0}\int_t^{t+T_0} \Phi\Phi^\top \mathrm{d}\tau \ge \frac{\alpha_0}{m_0} T_0 I,\ \forall t \ge 0 \tag{50}$$

for some $\alpha_0, T_0 > 0$, where $m_0 = \sup_\ell m_s^2(\ell)$, which implies that $\frac{\Phi}{m_s}$ is persistently exciting. From (46), we have

$$V(t+T) = V(t) - \int_t^{t+T} \varepsilon^2 m_s^2 \mathrm{d}\ell = V(t) - \int_t^{t+T} \frac{\left(\tilde{\Theta}(\ell)\,\Phi(\ell)\right)^2}{m_s^2(\ell)}\mathrm{d}\ell \tag{51}$$

for any $t, T > 0$. Consider the identity

$$\tilde{\Theta}^\top(\ell)\frac{|\Phi(\ell)|}{m_s(\ell)} = \tilde{\Theta}^\top(t)\frac{|\Phi(\ell)|}{m_s(\ell)} + \left(\tilde{\Theta}(\ell) - \tilde{\Theta}(t)\right)^\top \frac{|\Phi(\ell)|}{m_s(\ell)}. \tag{52}$$

Using the inequality $(x+y)^2 \geq \frac{1}{2}x^2 - y^2$, we have

$$\begin{aligned}
&\int_t^{t+T}\left(\tilde{\Theta}^\top(\ell)\,\frac{|\Phi(\ell)|}{m_s(\ell)}\right)^2 \mathrm{d}\ell \\
&\quad=\int_t^{t+T}\left(\tilde{\Theta}^\top(t)\,\frac{|\Phi(\ell)|}{m_s(\ell)}+\left(\tilde{\Theta}(\ell)-\tilde{\Theta}(t)\right)^\top\frac{|\Phi(\ell)|}{m_s(\ell)}\right)^2 \mathrm{d}\ell \\
&\quad\geq \frac{1}{2}\int_t^{t+T}\left(\tilde{\Theta}^\top(t)\,\frac{|\Phi(\ell)|}{m_s(\ell)}\right)^2 \mathrm{d}\ell - \int_t^{t+T}\left(\left(\tilde{\Theta}(\ell)-\tilde{\Theta}(t)\right)^\top\frac{|\Phi(\ell)|}{m_s(\ell)}\right)^2 \mathrm{d}\ell.
\end{aligned} \tag{53}$$

Let us take $T = T_0$ in (51), (53) and consider each term in (53) separately. The first term satisfies

$$\begin{aligned}
&\frac{1}{2}\int_t^{t+T_0}\left(\tilde{\Theta}^\top(t)\,\frac{|\Phi(\ell)|}{m_s(\ell)}\right)^2 \mathrm{d}\ell \\
&\quad=\frac{1}{2}\tilde{\Theta}^\top(t)\left(\int_t^{t+T_0}\frac{|\Phi(\ell)|}{m_s(\ell)}\left(\frac{|\Phi(\ell)|}{m_s(\ell)}\right)^\top \mathrm{d}\ell\right)\tilde{\Theta}(t) \\
&\quad\geq \frac{\alpha_0}{2}T_0\tilde{\Theta}^\top(t)\,\tilde{\Theta}(t) \geq \alpha_0 T_0\lambda_{\min}(F)\,V(t).
\end{aligned} \tag{54}$$

For the second term on the right-hand side of (53), we use

$$\begin{aligned}
\tilde{\Theta}(\ell)-\tilde{\Theta}(t) &= \int_t^\ell \dot{\tilde{\Theta}}(\sigma)\,\mathrm{d}\sigma = \int_t^\ell F\varepsilon\Phi \mathrm{d}\sigma \\
&= -\int_t^\ell F\tilde{\Theta}^\top(\sigma)\,\frac{|\Phi(\sigma)|}{m_s(\sigma)}\frac{|\Phi(\sigma)|}{m_s(\sigma)}\mathrm{d}\sigma.
\end{aligned} \tag{55}$$

Then

$$\begin{aligned}
&\left[\tilde{\Theta}(\ell)-\tilde{\Theta}(t)\right]^\top\frac{|\Phi(\ell)|}{m_s(\ell)} \\
&\quad=-\int_t^\ell \tilde{\Theta}^\top(\sigma)\,\frac{|\Phi(\sigma)|}{m_s(\sigma)}\left(\frac{|\Phi(\ell)|}{m_s(\ell)}\right)^\top F\frac{|\Phi(\sigma)|}{m_s(\sigma)}\mathrm{d}\sigma.
\end{aligned} \tag{56}$$

Using Schwarz inequality, the second term in (53) with $T = T_0$ satisfies

$$\begin{aligned}
&\int_t^{t+T_0}\left(\left[\tilde{\Theta}(\ell)-\tilde{\Theta}(t)\right]^\top\frac{|\Phi(\ell)|}{m_s(\ell)}\right)^2 \mathrm{d}\ell \\
&=\int_t^{t+T_0}\left(\int_t^\ell \tilde{\Theta}^\top(\sigma)\,\frac{|\Phi(\sigma)|}{m_s(\sigma)}\frac{|\Phi^\top(\ell)|}{m_s(\ell)}F\frac{|\Phi(\sigma)|}{m_s(\sigma)}\mathrm{d}\sigma\right)^2 \mathrm{d}\ell \\
&\leq\int_t^{t+T_0}\left(\int_t^\ell\left(\frac{|\Phi^\top(\sigma)|}{m_s(\sigma)}F\frac{|\Phi(\sigma)|}{m_s(\sigma)}\right)^2\mathrm{d}\sigma\int_t^\ell\left(\tilde{\Theta}^\top(\sigma)\,\frac{|\Phi(\sigma)|}{m_s(\sigma)}\right)^2\mathrm{d}\sigma\right)\mathrm{d}\ell.
\end{aligned} \tag{57}$$

As $\frac{|\Phi|}{m_s} \in \mathcal{L}_\infty$, define the constant $\beta = \sup_{\ell\geq 0}|\frac{|\Phi(\ell)|}{m_s(\ell)}|$. We get

$$\begin{aligned}
&\int_t^{t+T_0}\left(\left(\tilde{\Theta}(\ell)-\tilde{\Theta}(t)\right)^\top\frac{|\Phi(\ell)|}{m_s(\ell)}\right)^2 \mathrm{d}\ell \\
&\leq \beta^4\lambda_{\max}^2(F)\int_t^{t+T_0}(\ell-t)\int_t^\ell\left(\tilde{\Theta}^\top(\sigma)\,\frac{|\Phi(\sigma)|}{m_s(\sigma)}\right)^2\mathrm{d}\sigma\mathrm{d}\ell \\
&= \beta^4\lambda_{\max}^2(F)\int_t^{t+T_0}\left(\tilde{\Theta}^\top(\sigma)\,\frac{|\Phi(\sigma)|}{m_s(\sigma)}\right)^2\int_t^{t+T_0}(\ell-t)\,\mathrm{d}\ell\mathrm{d}\sigma \\
&= \beta^4\lambda_{\max}^2(F)\int_t^{t+T_0}\left(\tilde{\Theta}^\top(\sigma)\,\frac{|\Phi(\sigma)|}{m_s(\sigma)}\right)^2\left(\frac{T_0^2-(\sigma-t)^2}{2}\right)\mathrm{d}\sigma \\
&\leq \beta^4\lambda_{\max}^2(F)\,\frac{T_0^2}{2}\int_t^{t+T_0}\left(\tilde{\Theta}^\top(\sigma)\,\frac{|\Phi(\sigma)|}{m_s(\sigma)}\right)^2\mathrm{d}\sigma.
\end{aligned} \tag{58}$$

Using (54), (58) in (53) with $T = T_0$ we have

$$\begin{aligned}
&\int_t^{t+T_0}\left(\tilde{\Theta}^\top(\ell)\,\frac{|\Phi(\ell)|}{m_s(\ell)}\right)^2 \mathrm{d}\ell \geq \\
&\alpha_0 T_0\lambda_{\min}(F)\,V(t) - \beta^4\lambda_{\max}^2(F)\,\frac{T_0^2}{2}\int_t^{t+T_0}\left(\tilde{\Theta}^\top(\ell)\,\frac{|\Phi(\ell)|}{m_s(\ell)}\right)^2\mathrm{d}\ell,
\end{aligned} \tag{59}$$

which implies

$$\begin{aligned}
\int_t^{t+T_0}\left(\tilde{\Theta}^\top\frac{|\Phi(\ell)|}{m_s(\ell)}\right)^2\mathrm{d}\ell &\geq \frac{2\alpha_0 T_0\lambda_{\min}(F)}{2+\beta^4\lambda_{\max}^2(F)\,T_0^2}V(t) \\
&= \gamma_1 V(t),
\end{aligned} \tag{60}$$

where $\gamma_1 = \frac{2\alpha_0 T_0\lambda_{\min}(F)}{2+\beta^4\lambda_{\max}^2(F)T_0^2}$. Using (60) in (51) with $T = T_0$, we have

$$V(t+T_0) \leq V(t) - \gamma_1 V(t) = (1-\gamma_1)\,V(t). \tag{61}$$

Since $\gamma_1 > 0$ and $V(t+T_0) \geq 0$ it follows that $0 < \gamma_1 < 1$. Since (61) holds for all $t \geq 0$ we can take $t = (n-1)\,T_0$, where $n = 0, 1, 2, 3, \ldots$, to obtain

$$\begin{aligned}
V(t) \leq V(nT_0) &\leq (1-\gamma_1)\,V((n-1)\,T_0) \\
&\leq \ldots \leq (1-\gamma_1)^n\,V(0)
\end{aligned} \tag{62}$$

$\forall t \geq nT_0$. Hence $V(t) \to 0$ as $t \to \infty$ exponentially, which implies that $\Theta(t) \to \Theta^*$ exponentially. This concludes the proof.

## REFERENCES


[1] S. Eilers, J. Mårtensson, H. Pettersson, M. Pillado, D. Gallegos, M. Tobar, K. H. Johansson, X. Ma, T. Friedrichs, S. S. Borojeni, and M. Adolfson, "COMPANION – towards co-operative platoon management of heavy-duty vehicles," in *2015 IEEE 18th International Conference on Intelligent Transportation Systems*, 2015, pp. 1267–1273.

[2] Y. Xue, C. Ding, B. Yu, and W. Wang, "A platoon-based hierarchical merging control for on-ramp vehicles under connected environment," *IEEE Transactions on Intelligent Transportation Systems*, vol. 23, no. 11, pp. 21 821–21 832, 2022.

[3] Y. Zhang, Z. Wu, Y. Zhang, Z. Shang, P. Wang, Q. Zou, X. Zhang, and J. Hu, "Human-lead-platooning cooperative adaptive cruise control," *IEEE Transactions on Intelligent Transportation Systems*, vol. 23, no. 10, pp. 18 253–18 272, 2022.

[4] J. Ploeg, D. P. Shukla, N. van de Wouw, and H. Nijmeijer, "Controller synthesis for string stability of vehicle platoons," *IEEE Transactions on Intelligent Transportation Systems*, vol. 15, no. 2, pp. 854–865, 2014.

[5] Y. Li, W. Chen, S. Peeta, and Y. Wang, "Platoon control of connected multi-vehicle systems under V2X communications: Design and experiments," *IEEE Transactions on Intelligent Transportation Systems*, vol. 21, no. 5, pp. 1891–1902, 2020.

[6] G. Gunter, D. Gloudemans, R. E. Stern, S. McQuade, R. Bhadani, M. Bunting, M. L. Delle Monache, R. Lysecky, B. Seibold, J. Sprinkle, B. Piccoli, and D. B. Work, "Are commercially implemented adaptive cruise control systems string stable?" *IEEE Transactions on Intelligent Transportation Systems*, vol. 22, no. 11, pp. 6992–7003, 2021.

[7] J. Ploeg, N. van de Wouw, and H. Nijmeijer, "Lp string stability of cascaded systems: Application to vehicle platooning," *IEEE Transactions on Control Systems Technology*, vol. 22, no. 2, pp. 786–793, 2014.

[8] V. S. Dolk, J. Ploeg, and W. P. M. H. Heemels, "Event-triggered control for string-stable vehicle platooning," *IEEE Transactions on Intelligent Transportation Systems*, vol. 18, no. 12, pp. 3486–3500, 2017.

[9] Y. Li, B. Chen, H. Zhao, S. Peeta, S. Hu, Y. Wang, and Z. Zheng, "A car-following model for connected and automated vehicles with heterogeneous time delays under fixed and switching communication topologies," *IEEE Transactions on Intelligent Transportation Systems*, vol. 23, no. 9, pp. 14 846–14 858, 2022.

[10] H. Rezaee, K. Zhang, T. Parisini, and M. M. Polycarpou, "Cooperative adaptive cruise control in the presence of communication and radar stochastic data loss," *IEEE Transactions on Intelligent Transportation Systems*, vol. 25, no. 6, pp. 4964–4976, 2024.

[11] H. Xing, J. Ploeg, and H. Nijmeijer, "Compensation of communication delays in a cooperative acc system," *IEEE Transactions on Vehicular Technology*, vol. 69, no. 2, pp. 1177–1189, 2020.

[12] S. Öncü, J. Ploeg, N. van de Wouw, and H. Nijmeijer, "Cooperative adaptive cruise control: Network-aware analysis of string stability," *IEEE Transactions on Intelligent Transportation Systems*, vol. 15, no. 4, pp. 1527–1537, 2014.

[13] J. Ploeg, E. Semsar-Kazerooni, G. Lijster, N. van de Wouw, and H. Nijmeijer, "Graceful degradation of cooperative adaptive cruise control," *IEEE Transactions on Intelligent Transportation Systems*, vol. 16, no. 1, pp. 488–497, 2015.

[14] F. Acciani, P. Frasca, G. Heijenk, and A. A. Stoorvogel, "Stochastic string stability of vehicle platoons via cooperative adaptive cruise control with lossy communication," *IEEE Transactions on Intelligent Transportation Systems*, vol. 23, no. 8, pp. 10 912–10 922, 2022.

[15] Q. Chen, Y. Zhou, S. Ahn, J. Xia, S. Li, and S. Li, "Robustly string stable longitudinal control for vehicle platoons under communication failures: A generalized extended state observer-based control approach," *IEEE Transactions on Intelligent Vehicles*, vol. 8, no. 1, pp. 159–171, 2023.

[16] J. Lunze, "Adaptive cruise control with guaranteed collision avoidance," *IEEE Transactions on Intelligent Transportation Systems*, vol. 20, no. 5, pp. 1897–1907, 2019.

[17] A. Schwab and J. Lunze, "Design of platooning controllers that achieve collision avoidance by external positivity," *IEEE Transactions on Intelligent Transportation Systems*, vol. 23, no. 9, pp. 14 883–14 892, 2022.

[18] Y. A. Harfouch, S. Yuan, and S. Baldi, "An adaptive switched control approach to heterogeneous platooning with intervehicle communication losses," *IEEE Transactions on Control of Network Systems*, vol. 5, no. 3, pp. 1434–1444, 2018.

[19] M. P. Silva de Abreu, F. S. S. de Oliveira, and F. de Oliveira Souza, "d-CACC for vehicle platoons lacking acceleration signal," *IEEE Transactions on Intelligent Transportation Systems*, vol. 25, no. 8, pp. 9028–9038, 2024.

[20] V. Vegamoor, S. Rathinam, and S. Darbha, "String stability of connected vehicle platoons under lossy V2V communication," *IEEE Transactions on Intelligent Transportation Systems*, vol. 23, no. 7, pp. 8834–8845, 2022.

[21] H. M. Wang, S. S. Avedisov, O. Altintas, and G. Orosz, "Multi-vehicle conflict management with status and intent sharing under time delays," *IEEE Transactions on Intelligent Vehicles*, vol. 8, no. 2, pp. 1624–1637, 2023.

[22] H. M. Wang, S. S. Avedisov, T. G. Molnár, A. H. Sakr, O. Altintas, and G. Orosz, "Conflict analysis for cooperative maneuvering with status and intent sharing via V2X communication," *IEEE Transactions on Intelligent Vehicles*, vol. 8, no. 2, pp. 1105–1118, 2023.

[23] H. M. Wang, S. S. Avedisov, O. Altintas, and G. Orosz, "Intent sharing in cooperative maneuvering: Theory and experimental evaluation," *IEEE Transactions on Intelligent Transportation Systems*, vol. 25, no. 9, pp. 12 450–12 463, 2024.

[24] J. Sawant, U. Chaskar, and D. Ginoya, "Robust control of cooperative adaptive cruise control in the absence of information about preceding vehicle acceleration," *IEEE Transactions on Intelligent Transportation Systems*, vol. 22, no. 9, pp. 5589–5598, 2021.

[25] T. Keijzer and R. M. Ferrari, "Threshold design for fault detection with first order sliding mode observers," *Automatica*, vol. 146, p. 110600, 2022.

[26] D. Liu, S. Mair, K. Yang, S. Baldi, P. Frasca, and M. Althoff, "Resilience in platoons of cooperative heterogeneous vehicles: Self-organization strategies and provably-correct design," *IEEE Transactions on Intelligent Vehicles*, vol. 9, no. 1, pp. 2262–2275, 2024.

[27] J. Yang, D. Chu, J. Yin, D. Pi, J. Wang, and L. Lu, "Distributed model predictive control for heterogeneous platoon with leading human-driven vehicle acceleration prediction," *IEEE Transactions on Intelligent Transportation Systems*, vol. 25, no. 5, pp. 3944–3959, 2024.

[28] X. Jin, W. M. Haddad, and T. Yucelen, "An adaptive control architecture for mitigating sensor and actuator attacks in cyber-physical systems," *IEEE Transactions on Automatic Control*, vol. 62, no. 11, pp. 6058–6064, 2017.

[29] K. Yang, D. Liu, S. Baldi, W. Yu, and C. Lv, "Decoupling-based resilient control of vehicular platoons under injection of false wireless data," *IEEE Transactions on Intelligent Transportation Systems*, pp. 1–15, 2024.

[30] M. Zhang, Z. Liu, and H. Su, "Robust adaptive output regulation for EV dynamic wireless charging system with sinusoidal disturbance of unknown frequency," *IEEE Transactions on Industrial Electronics*, vol. 71, no. 7, pp. 7301–7311, 2024.

[31] C. Deng, D. Zhang, and G. Feng, "Resilient practical cooperative output regulation for mass with unknown switching exosystem dynamics under DoS attacks," *Automatica*, vol. 139, p. 110172, 2022.

[32] A. Isidori, L. Marconi, and A. Serrani, *Robust autonomous guidance: an internal model approach*. Springer Science & Business Media, 2003.

[33] J. Huang and Z. Chen, "A general framework for tackling the output regulation problem," *IEEE Transactions on Automatic Control*, vol. 49, no. 12, pp. 2203–2218, 2004.

[34] T. Liu, S. Wang, and J. Huang, "An adaptive distributed observer for a class of uncertain linear leader systems over jointly connected switching networks and its application," *IEEE Transactions on Automatic Control*, vol. 69, no. 11, pp. 7340–7355, 2024.

[35] W. Liu and J. Huang, "Output regulation of linear systems via sampled-data control," *Automatica*, vol. 113, p. 108684, 2020.

[36] G. J. L. Naus, R. P. A. Vugts, J. Ploeg, M. J. G. van de Molengraft, and M. Steinbuch, "String-stable CACC design and experimental validation: A frequency-domain approach," *IEEE Transactions on Vehicular Technology*, vol. 59, no. 9, pp. 4268–4279, 2010.

[37] Y. Zhou and S. Ahn, "Robust local and string stability for a decentralized car following control strategy for connected automated vehicles," *Transportation Research Part B: Methodological*, vol. 125, pp. 175–196, 2019.

[38] S. Baldi, D. Liu, V. Jain, and W. Yu, "Establishing platoons of bidirectional cooperative vehicles with engine limits and uncertain dynamics," *IEEE Transactions on Intelligent Transportation Systems*, vol. 22, no. 5, pp. 2679–2691, 2021.

[39] P. Barooah and J. Hespanha, "Error amplification and disturbance propagation in vehicle strings with decentralized linear control," in *Proceedings of the 44th IEEE Conference on Decision and Control*, 2005, pp. 4964–4969.

[40] P. Wijnbergen and B. Besselink, "Existence of decentralized controllers for vehicle platoons: On the role of spacing policies and available measurements," *Systems & Control Letters*, vol. 145, p. 104796, 2020.

[41] D. Liu, B. Besselink, S. Baldi, W. Yu, and H. L. Trentelman, "An adaptive disturbance decoupling perspective to longitudinal platooning," *IEEE Control Systems Letters*, vol. 6, pp. 668–673, 2022.

[42] D. Liu, S. Baldi, and S. Hirche, "Collision avoidance in longitudinal platooning: Graceful degradation and adaptive designs," *IEEE Control Systems Letters*, vol. 7, pp. 1694–1699, 2023.

[43] A. Astolfi and L. Marconi, *Analysis and Design of Nonlinear Control Systems*. Springer, 2008.

[44] D. Cheng, X. Hu, and T. Shen, *Analysis and design of nonlinear control systems*. Springer, 2010.

[45] D. Carnevale, S. Galeani, L. Menini, and M. Sassano, "Hybrid output regulation for linear systems with periodic jumps: Solvability conditions,

structural implications and semi-classical solutions," *IEEE Transactions on Automatic Control*, vol. 61, no. 9, pp. 2416–2431, 2016.
[46] K. Zheng, Q. Zheng, P. Chatzimisios, W. Xiang, and Y. Zhou, "Heterogeneous vehicular networking: A survey on architecture, challenges, and solutions," *IEEE Communications Surveys & Tutorials*, vol. 17, no. 4, pp. 2377–2396, 2015.
[47] M. A. Khan, S. Ghosh, S. A. Busari, K. M. S. Huq, T. Dagiuklas, S. Mumtaz, M. Iqbal, and J. Rodriguez, "Robust, resilient and reliable architecture for V2X communications," *IEEE Transactions on Intelligent Transportation Systems*, vol. 22, no. 7, pp. 4414–4430, 2021.
[48] F. Abbas, P. Fan, and Z. Khan, "A novel low-latency V2V resource allocation scheme based on cellular V2X communications," *IEEE Transactions on Intelligent Transportation Systems*, vol. 20, no. 6, pp. 2185–2197, 2019.
[49] X. Li, L. Ma, R. Shankaran, Y. Xu, and M. A. Orgun, "Joint power control and resource allocation mode selection for safety-related V2X communication," *IEEE Transactions on Vehicular Technology*, vol. 68, no. 8, pp. 7970–7986, 2019.
[50] R. Krajewski, J. Bock, L. Kloeker, and L. Eckstein, "The highD dataset: A drone dataset of naturalistic vehicle trajectories on German highways for validation of highly automated driving systems," in *2018 21st International Conference on Intelligent Transportation Systems (ITSC)*, 2018, pp. 2118–2125.
[51] M. Boban, A. Kousaridas, K. Manolakis, J. Eichinger, and W. Xu, "Connected roads of the future: Use cases, requirements, and design considerations for vehicle-to-everything communications," *IEEE Vehicular Technology Magazine*, vol. 13, no. 3, pp. 110–123, 2018.
[52] V. Maglogiannis, D. Naudts, S. Hadiwardoyo, D. van den Akker, J. Marquez-Barja, and I. Moerman, "Experimental V2X evaluation for C-V2X and ITS-G5 technologies in a real-life highway environment," *IEEE Transactions on Network and Service Management*, vol. 19, no. 2, pp. 1521–1538, 2022.
[53] M. Pirani, E. Hashemi, J. W. Simpson-Porco, B. Fidan, and A. Khajepour, "Graph theoretic approach to the robustness of $k$ -nearest neighbor vehicle platoons," *IEEE Transactions on Intelligent Transportation Systems*, vol. 18, no. 11, pp. 3218–3224, 2017.
[54] C. K. Verginis, C. P. Bechlioulis, D. V. Dimarogonas, and K. J. Kyriakopoulos, "Robust distributed control protocols for large vehicular platoons with prescribed transient and steady-state performance," *IEEE Transactions on Control Systems Technology*, vol. 26, no. 1, pp. 299–304, 2018.
[55] A. C. Pandey and S. B. Roy, "Composite adaptive control of heterogeneous vehicle platoon with a virtual platoon based stability analysis," in *2025 IEEE Intelligent Vehicles Symposium (IV)*, 2025, pp. 1705–1711.
[56] E. Arabi and T. Yucelen, "Set-theoretic model reference adaptive control with time-varying performance bounds," *International Journal of Control*, vol. 92, no. 11, pp. 2509–2520, 2019.
[57] M. Green and J. B. Moore, "Persistence of excitation in linear systems," *Systems & Control Letters*, vol. 7, no. 5, pp. 351–360, 1986.
[58] A. Padoan, G. Scarciotti, and A. Astolfi, "A geometric characterization of the persistence of excitation condition for the solutions of autonomous systems," *IEEE Transactions on Automatic Control*, vol. 62, no. 11, pp. 5666–5677, 2017.

**Jing Li** is currently working towards her PhD degree through a joint program between Southeast University and The Hong Kong Polytechnic University. Her research interests include modeling of microscopic traffic and connected automated vehicles.

**Di Liu** (M'22) received a first Ph.D. in cyber science and engineering from Southeast University, China, in 2021, and a second Ph.D. in systems and control from the University of Groningen, The Netherlands, in 2022. She was a Joint Marie Sklodowska Curie Fellow with the Technical University of Munich, Germany, and Ecole Polytechnique Federale de Lausanne (EPFL), Switzerland, from 2022 to 2024. She is currently a Marie Sklodowska Curie Fellow & UKRI Fellow with Imperial College London, UK. Her research interests include learning systems and control, with application in intelligent transportation, and autonomous and connected vehicles.

**Simone Baldi** (M'14, SM'19) received the B.Sc. in electrical engineering, and the M.Sc. and Ph.D. in automatic control engineering from University of Florence, Italy, in 2005, 2007, and 2011, respectively. He is professor at Southeast University, previously being assistant professor at Delft Center for Systems and Control, TU Delft. He was awarded outstanding reviewer of *Applied Energy* (2016) and *Automatica* (2017). He is subject editor of *International Journal of Adaptive Control and Signal Processing*, senior editor of *IEEE Control Systems Letters* and technical editor of *IEEE/ASME Trans. on Mechatronics*. His research interests include adaptive and learning systems with applications in networked systems and intelligent vehicles.

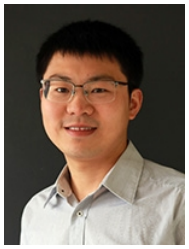

**Wei Liu** is currently the Associate Head and Associate Professor at the Department of Aeronautical and Aviation Engineering, The Hong Kong Polytechnic University. Before this, he was a faculty member at University of New South Wales, Sydney in Australia and University of Glasgow in the United Kingdom. Dr. Liu earned his PhD in Transportation from the Hong Kong University of Science and Technology in 2014, and his B.Eng. in Civil Engineering and Bachelor of Laws from Tsinghua University in 2010. He is a recipient of the Discovery Early Career Researcher Award from the Australian Research Council. His research focuses on data-driven decision analytics; large-scale transport system modeling, optimization and computing; aviation and rail system modeling; and transport economics.